Adsorption of Triblock Copolymers on Rough Surfaces

Anna C. Balazs* and Kanglin Huang

Materials Science and Engineering Department, University of Pittsburgh, Pittsburgh, Pennsylvania 15261

Christopher W. Lantman

Mobay Corporation, Bayer USA Inc., Pittsburgh, Pennsylvania 15205-9741

Received January 26, 1990; Revised Manuscript Received April 4, 1990

ABSTRACT: We examine the adsorption of ABA triblocks in solution onto a rough, corrugated surface. The solution is assumed to be a good solvent for the B block and a bad solvent for the A segments. Solvent incompatibility drives the A blocks to adsorb onto the nearest interface. We find that, under favorable conditions, the A moieties bind to the ridges of the bumpy surface and the B segments span the wells that lie between two ridges. Consequently, the adsorption of triblocks acts to smooth or planarize a rough surface. We discuss how chain length and the value of χ_{BS}, the interaction energy between the B block and the surface, affect the efficiency of this process.

Introduction

The problem of polymer adsorption on rough surfaces has attracted considerable attention in recent years.[1-3] This problem poses questions not only of scientific interest but also of technological importance. In the past, several investigations have focused on polymer adsorption onto flat surfaces.[4] Since few real surfaces are microscopically smooth, determining how the surface topology modifies the adsorption process is of significant interest. Current work in this area has been concerned with the adsorption of homopolymers on a variety of surfaces, including sinusoidal curves[1,2] and fractal interfaces.[3] In this paper, we will use Monte Carlo computer simulations to examine the surface adsorption of ABA triblock copolymers on uniformly corrugated surfaces. Here, we assume the molecules adsorb from a solution that is a poor solvent for the A segment but a good solvent for the B block.

We have chosen this system for two principal reasons. First, in a recent paper,[5] we have examined the adsorption of such ABA triblocks onto a flat surface. Thus, by comparing the previous results with our new findings, we can determine how variations in surface structure affect the adsorption of these molecules. Second, such a triblock architecture would intuitively seem appropriate for smoothing or planarizing rough surfaces: the solvent-compatible A segments will adsorb onto ridges in the surface, while the solvent-compatible B segment can span the wells or troughs that occur between these ridges. The extent to which this phenomenon occurs and the factors that affect the process are examined in this paper. To accomplish this goal, we observed the adsorption of various ABA copolymers onto a bumpy surface of fixed geometry (see Figure 1). In particular, we varied the length of the intervening B block, altered the interaction energy between the B segment and the surface, and contrasted our copolymer results with the behavior of a homopolymer on the same rough surface.

The results from these calculations may have significant technological applications, particularly in the coatings industry and in the fabrication of integrated circuits. A parameter that is critical for the fabrication of submicron structures is the flatness of the surface, or planarity.[6] The adsorption of triblock copolymers could be useful as one of the processing steps in the planarization of such surfaces.

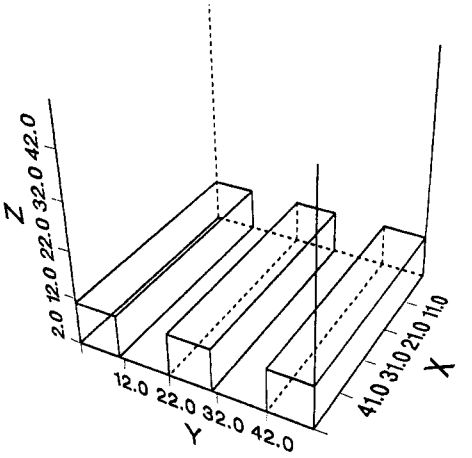

Figure 1. View of the corrugated surface.

The Model

The simulation is started by placing 20 self-avoiding random walk chains at random locations in a cubic box that is $50 \times 50 \times 50$ lattice sites in size. For the simulation of adsorption onto a smooth surface, the bottom of the box is flat and is defined by the $Z = 1$ plane. The first layer of the polymer film is contained in the $Z = 2$ plane. In contrast, the simulation of a rough surface uses a corrugated box as shown in Figure 1. Each corrugation or bump is 10 lattice sites high and 10 lattice sites wide. Polymers can adsorb anywhere on this corrugated interface, namely, in the wells ($Z = 2$–11) and on the top of the bumps ($Z = 12$).

The chains have two "sticky" beads at each end: these model the A segments of the polymer. As noted above, the case we are simulating is one in which the solution is a poor solvent for the A moiety. Thus, solvent incompatibility drives these units to bind to the nearest interface. The length of the A block is held fixed at two lattice sites. The length of the entire chain, N, is varied by altering the length of the solvent-compatible B block.

The chains diffuse through the box via translating and "wiggling" motions. In particular, the entire chain is translated one lattice site in one of six directions chosen at random. Then the chain is wiggled by using the algorithm for chain dynamics developed by Verdier and Stockmayer[7] and Hilhorst and Deutch.[8] All attempted moves must obey the excluded-volume criteria.

0024-9297/90/2223-4641$02.50/0

The chains continue to diffuse until an A bead is one lattice unit above any surface site. Then, the A bead remains bound at this location, while the remainder of the chain is free to wiggle about this point of attachment. Whenever any A bead is one lattice site above the surface, it binds at that location, thus modeling the strong affinity between an A monomer and the surface. When both ends of the chain are bound, the intervening B units are still allowed to wiggle between these two fixed points (under the constraint that the chain does not break at any time). Thus, even if a B segment now comes in contact with a surface site, in a later move, it can wiggle away from its surface location. This aspect of the program models the weak B-surface interaction and the strong B-solvent affinity.

Whenever a free chain binds to the surface, a new chain is added to the solution, thus keeping the number of chains in the bath constant. Here, the solution acts as an infinite source of free chains.

In the simulations described above, we assumed that the binding between the surface and the A moieties is irreversible. There is considerable experimental evidence to validate this assumption for comparable systems.[9] To investigate the effect reversible surface adsorption has on our observations, another simulation was implemented. Here, in a later time step, a bound chain can break away from the surface with a prescribed probability P. Thus, the polymer–surface bond has a finite lifetime, τ, which is inversely proportional to P.[10] The results from these simulations are also discussed.

The simulations were performed in two and three dimensions. All the reported data are from the 3D models. The 2D models were used to generate figures from which one can develop a qualitative understanding for the complicated surface-adsorption process. The data were collected after 6 million time steps. Here, the surface coverage has saturated, and running the program further results in the addition of one new chain only every 2 or 3 million time steps. All data points represent an average over three independent simulations.

In these investigations, we are focusing our attention on the nature of the polymer–surface interaction. Thus, we neglect A–A associations in the solution and between free and adsorbed chains. Such interactions can be neglected in the case of polymer adsorption from a dilute solution, where the probability of chain–chain contact is small. For more concentrated systems, the model is applicable in the case where the A–A association is energetically less favorable than the A–surface interaction. In previous studies, we examined the effects of A–A association on adsorption[5] and self-assembly.[11]

Finally, we note that since the bulk of the calculations were performed under the assumption that the binding between the stickers and the surface is irreversible, the study is primarily kinetic in nature. However, recent kinetic studies[12] indicate that while the initial surface adsorption of copolymers is rapid, the equilibrium adsorbance is reached at much longer times. Thus, experimental measurements may be more revealing of the kinetic behavior than the final equilibrium state. Consequently, understanding the kinetic effects may be extremely helpful in explaining observed trends.

Results and Discussion

In order to develop an understanding for the effect of surface geometry on adsorption, we compare the adsorption of the ABA triblocks on both a flat surface and the bumpy interface shown in Figure 1. The simulation was carried out for chain lengths of 10 and 50 lattice sites. For both chain lengths, the total number of chains adsorbed on the surface was higher for the case of the rough surface. This finding agrees with predictions made for the adsorption of polymers onto fractal interfaces[3] and onto a sphere that is curved toward the polymer solution.[2] In our investigations, the effect was more pronounced for the shorter chains. A 20% increase was observed (223 versus 185) for chain length 10, whereas only a 15% increase was observed for chain length 50 (79 versus 68). This increased adsorption on the rough surface is primarily due to the fact that this interface has a larger surface area than the flat plane and, thus, provides more binding sites onto which the chains can attach. Note that the total number of adsorbed chains decreases as the length of the polymer is increased, a point that we have discussed in a previous paper.[5] This effect is due to steric hindrance: the long polymers sterically hinder new chains from adsorbing onto the surface.

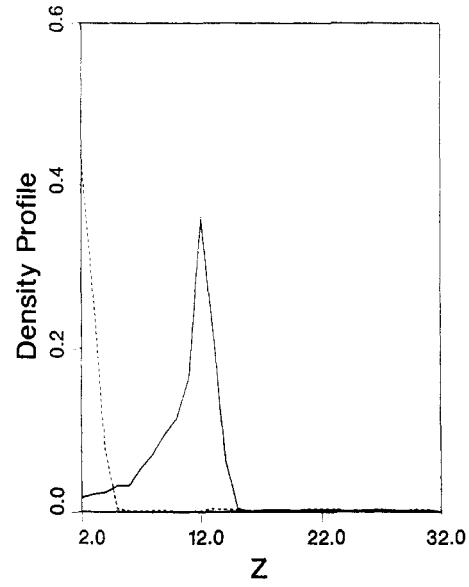

Figure 2. Segment density distribution (SDD) along the Z direction. The dashed line represents the density profile on the flat surface, while the solid line is the density profile on the rough surface. In both curves, $N = 10$.

Figure 2 shows the polymer segment density distribution (SDD) along the Z axis (normal to the plane of the surface) for both surface architectures and chain length equal to 10. As the solid line for the density distribution on the rough surface shows, there is a significant concentration of polymer in the wells (layers 2–11) between the bumps. The highest concentration of polymer is found on the top of the bumps ($Z = 12$). The dashed curve shows the polymer SDD on a flat surface for the same chain length. The maximum in this profile occurs on the surface layer ($Z = 2$) and is slightly higher than the other peak.

The average layer thickness can be estimated from these plots as the width of the curve at half its maximum height. The average layer thickness above the $Z = 12$ plane of the bumpy interface and the $Z = 2$ plane of the flat surface is approximately equal to 1 lattice unit. The maximum film thickness can be determined from the breadth of the SDD. In both curves, the film does not extend more than 5 lattice sites above these surfaces. In a previous article,[5] we noted that, for a chain length of 10, the majority of chains are in train conformations: contiguous segments that lie flat along the surface. This fact contributes to the compactness of the films atop both surface topologies.

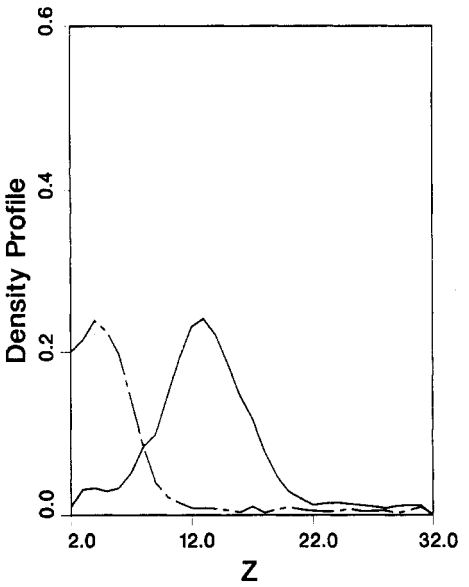

Figure 3. SDD along the Z direction for $N = 50$. The dashed line represents the density profile on the flat surface, while the solid line represents the density profile on the rough surface.

By examining the curves in Figure 3, we can make similar comparisons of the SDD for a chain length of 50 on both a rough and flat surface. The SDD for the flat surface (dashed line) shows that the maximum in polymer density lies a few layers away from the actual surface. This is due to the fact that the majority of these long chains are in "tail" or "loop" configurations, which lie away from the surface. The SDD for the rough interface (solid line) shows a greater amount of polymer on the top surface ($Z = 12$), and the maximum segment density lies closer to this plane. In addition, the width of the curve above $Z = 12$ narrows more rapidly than the width above $Z = 2$ in the dashed figure.

These differences can best be understood by viewing Figure 4, the output of the simulation on a bumpy surface in two dimensions. For long chains ($N = 40$), the sticky ends can bind to the edges of neighboring bumps, with the B segment spanning the well that lies between. Thus, the chain is effectively stretched between these two ridges. Consequently, the chain segments are more localized around the $Z = 12$ plane.

By comparison of Figures 2 and 3 and from the discussion above, we have observed that the effect of the surface roughness propagates into the layers above the bump height for the longer chain length.

To better understand the bridging phenomena displayed in Figure 4, we systematically varied the chain length in order to determine the critical length at which this behavior occurs and more generally, the effect of molecular weight on adsorption for a rough surface. Figure 5 shows the SDD along the Z direction for chain lengths 5, 20, and 30. (See Figures 2 and 3 for chain lengths 10 and 50, respectively.) Of particular interest is contrasting of the behavior in the well for various chain lengths. Since the bumps protrude from the bottom plane, a diffusing chain is more likely to encounter this surface first. Consequently, the chains have a higher probability of sticking to this interface. For chain lengths less than the width of the bump, the highest polymer density will be localized on the top of this surface. Thus, for chain length 5 (the dotted line in Figure 5), the distribution is sharply peaked around $Z = 12$: very little polymer has reached the bottom of the well; however, a certain amount is seen to coat the side of the bump between $Z = 8$ and 11. As the chain length is increased up to 20

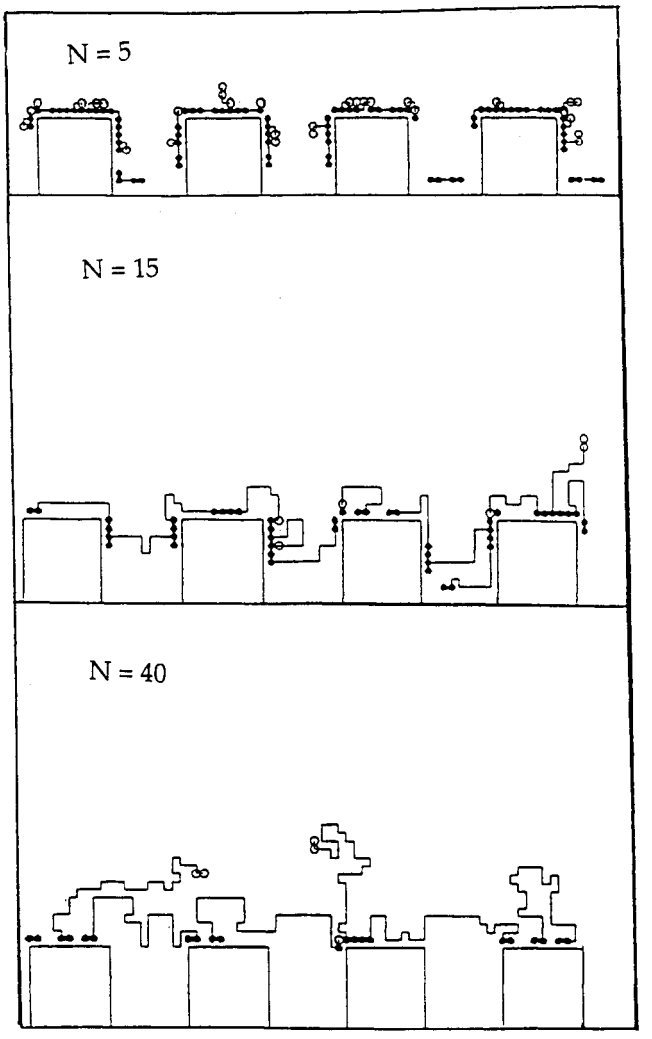

Figure 4. Output from the 2D simulations for chains 5, 15, and 40 lattice sites in length.

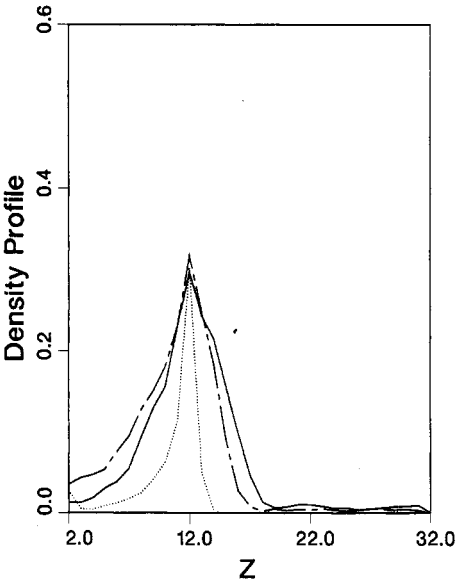

Figure 5. SDD along the Z direction for $N = 5$ (dotted line), $N = 20$ (dashed line), and $N = 30$ (solid line).

lattice sites (dashed line), more polymer is present in the well. Now, the chain is sufficiently long that one end may stick at or near the top of the bump, while the second sticky end can bind near or at the bottom. Increasing the chain length to 30 lattice sites alters this pattern, as is apparent from the solid curve in Figure 5. The height of the profile

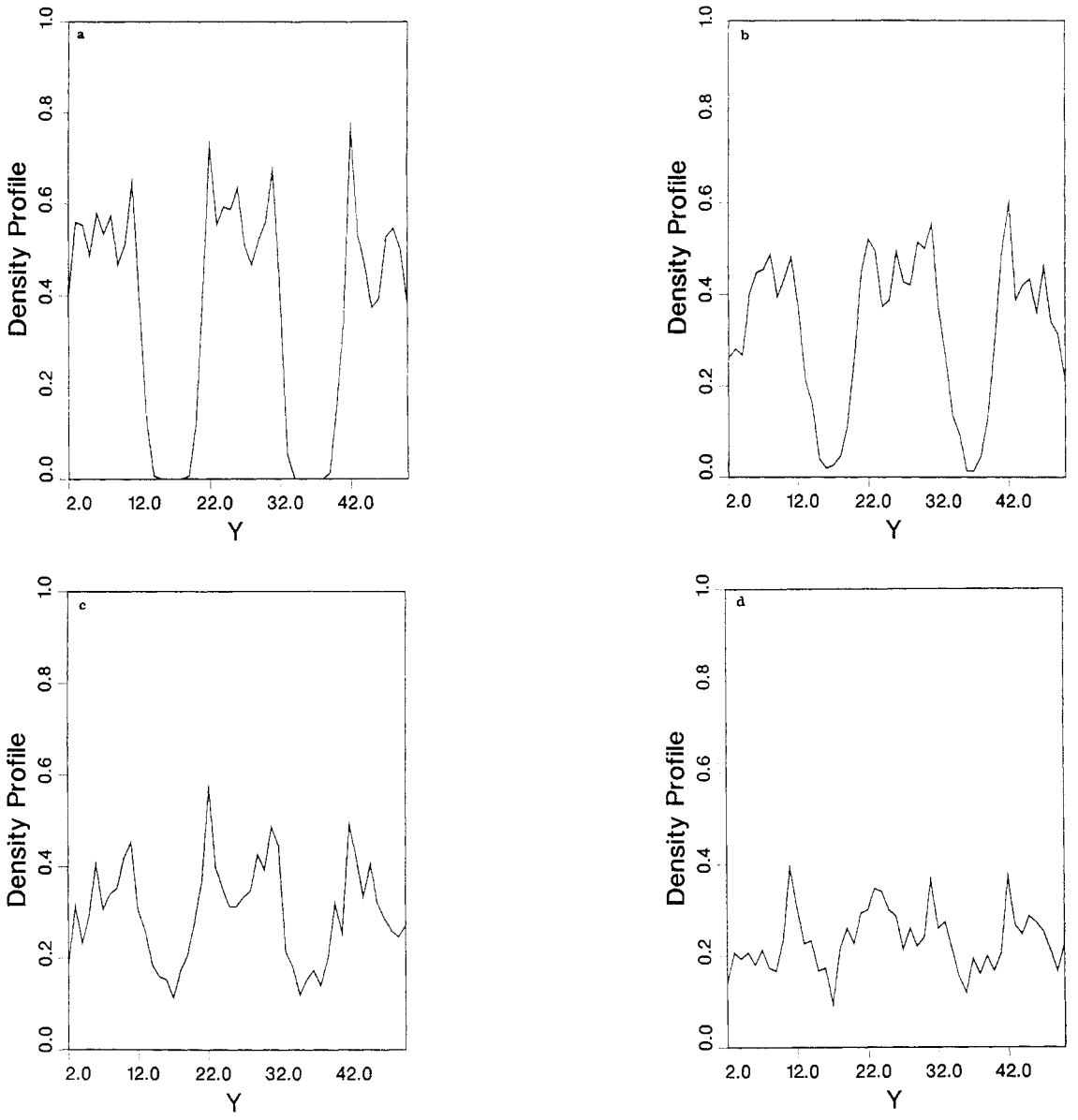

Figure 6. SDD along the Y direction and in the $Z = 12$ plane for (a) $N = 10$, (b) $N = 20$, (c) $N = 30$, and (d) $N = 50$.

for layers 2–11 is lower in the case for chain length 30 than it is for chain length 20. At this chain length, the ends of the chains bind to neighboring ridges and the chain can span the intervening well. As noted above, this localizes the polymer density closer to the $Z = 12$ plane. These observations are confirmed by the output from the 2D simulations in Figure 4.

It is of particular interest to further contrast the results for the longer chain lengths (30 and 50) in order to establish which candidate is more effective at this bridging behavior. To accomplish this goal, we will compare the polymer SDD directly above and parallel to the well: that is, along the Y direction and in the $Z = 12$ plane. Figure 6 shows this profile for $N = 10$, 20, 30, and 50. By comparing $N = 30$ and $N = 50$, we can see that there is a higher polymer density spanning the wells (which are located at $Y = 12$–22 and $Y = 32$–42) for the $N = 50$ case. Note the absence or decreased level of polymer in the regions between the wells for $N = 10$ and $N = 20$. Hence, the most effective bridging occurs for $N = 50$. This occurs because the mean end-to-end distance of the diffusing chain is comparable to the width of the well for $N = 50$. As a consequence, little or no chain deformation is required for the adsorption of each end onto adjacent bumps.

For several coating applications, it is important to know the surface coverage that results from a given adsorption process. We have evaluated surface coverage in the following way. First, the average film thickness is calculated as described above. Second, we examine the occupancy within this average layer by scanning along the Y direction. If a particular site (X, Y) is occupied in one or more of the horizontal planes that make up the average thickness, we consider the site to be covered and add a 1 to a running sum. We do this for each value of (X, Y) in the 50×50 plane and then divide our total by the area of the plane. This gives us an average surface coverage. The result of this calculation for the adsorption of chains with $N = 50$ is plotted in Figure 7. In this case, the average layer thickenss is 6 ($Z = 12$–17, inclusive) and the average surface coverage or polymer density in this film is equal to 56%. As can be seen from the figure, the 6-layer film provides appreciable coverage of the sites between the wells. The maximum density is still found above the bump height. For comparison, we repeated this calculation by using the total film thickness rather than the average. Including these additional layers in the calculation only increased the total surface coverage to 59%.

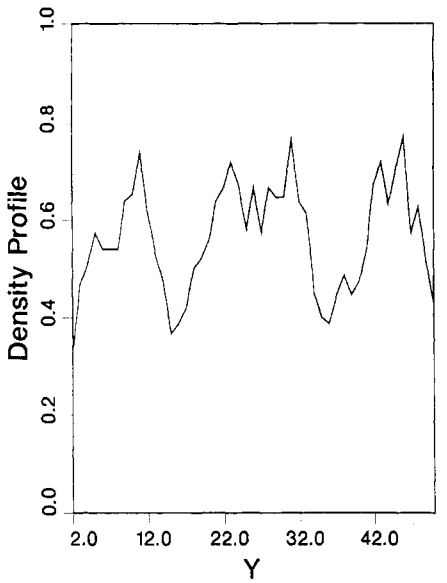

Figure 7. Polymer density along the Y direction for layers Z = 12–17, with N = 50. The average surface coverage equals 56%.

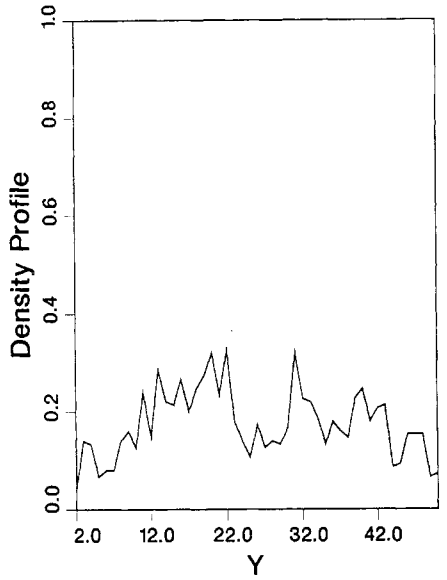

Figure 8. SDD along the Y direction and in the Z = 12 plane for N = 50 and χ_{BS} = 1.0.

In addition to surface coverage, it is important to determine the uniformity of the adsorbed film. A uniform coverage occurs when a high percentage of *contiguous* sites within the film are occupied. The degree of uniformity can be measured as the difference, d, between the maximum and minimum values in Figure 7. For the N = 50 case, d = 0.4.

In an effort to improve the uniformity of the film, we examined the surface adsorption of ABA molecules in which the interaction energy between a B segment and the surface is more repulsive. In this simulation, we again first check to see if an A segment is on top of a surface site; however, now the probability that the chain will stick is weighted by a factor $q = \exp(-n_B\chi_{BS})$, where n_B is the number of B segments also in contact with the surface and χ_{BS} is the interaction energy between the surface and a B site.[5] We investigated the case of χ_{BS} = 1.0 and N = 50. Figure 8 shows the SDD in the Y direction for the Z = 12 plane. Now, the highest polymer concentration is located in the region between the wells! Figure 9 shows the total SDD in the Y direction for the six layers, Z = 12–17, which again are comparable to the average layer

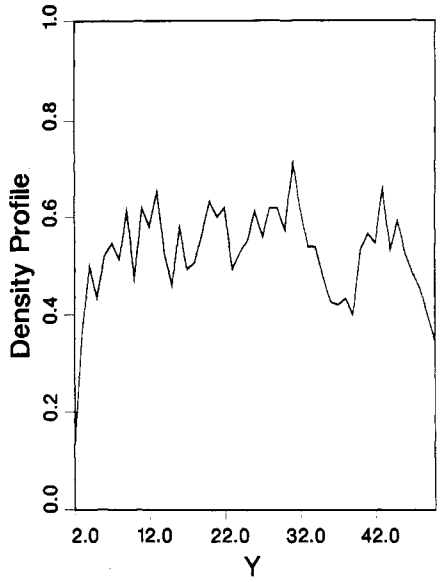

Figure 9. Polymer density, or surface coverage, along the Y direction for layers Z = 12–17, with N = 50 and χ_{BS} = 1.0. The average surface coverage is equal to 52%.

thickness. The average polymer density in this volume, 52%, is comparable to the previous case where N = 50 and χ_{BS} = 0.0; however, as the figure shows, the film is now more uniform. Here, the value of d is approximately 0.3, or a 30% difference between the minimum and maximum values in the curve. Again, the SDD normal to the Z direction extends another five layers above the average layer thickness. Including these layers into the calculation for the effective surface coverage increases the total value to 56%.

In effect, increasing χ_{BS} to 1.0 biased the chains away from positions along the area on top of the bump to the area above and between the wells, or in other words, into the solution, where the B-solvent interaction is more favorable. This establishes another important criterion in order for this bridging or planarizing behavior to be optimal: the A segments must be strongly attracted to the surface, while the B monomers should be strongly attracted to the solvent.

In order for the film of adsorbed ABA polymers to effectively decrease the surface roughness, two additional conditions must be met. First, a high, uniform coverage of the well and bump sites is required. A high occupancy of *contiguous* sites within the film layers will produce a uniform film. Second, the height of the polymer film *above* the average film thickness, or h_s, must be small. In other words, the protrusions above the adsorbed film must be small compared to the bump height. This requirement can be expressed mathematically by defining the degree of planarization as[13]

$$1 - h_s/h_b$$

where h_b is the bump height.

Among the copolymer examples studied here, the case for which χ_{BS} was equal to 1.0 yielded the most uniform films. Since the height of the bump was 10 lattice sites and h_s was equal to 5 lattice units, the degree of planarization is equal to 0.5, or 50%.

To establish whether the height of the bump affects our observations, we doubled the bump height to 20 lattice sites. Figure 10 shows the surface coverage provided by the average layer thickness when χ_{BS} = 1.0 and N = 50 (56% from layers Z = 22–27, inclusive). Though there is still appreciable coverage over the wells, the film is less

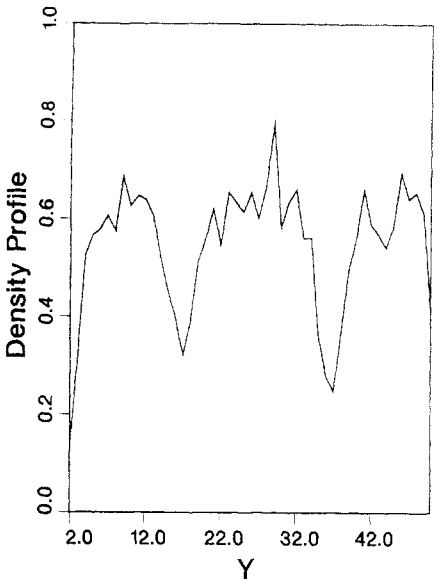

Figure 10. Polymer density along the Y direction for layers Z = 22–27, with N = 50, χ_{BS} = 1.0, and h_b = 20. The average surface coverage is equal to 56%.

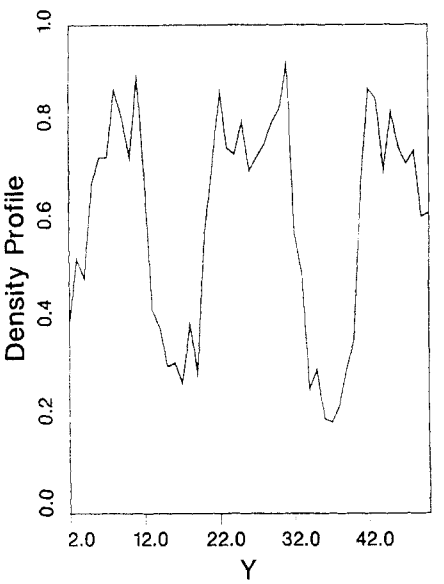

Figure 11. Homopolymer density along the Y direction for the layers Z = 12–14, with N = 50 and χ_{PS} = −1.0. The average surface coverage is 57%.

uniform here than in the h_b = 10 case. In particular, now d = 0.5. The general shape of the curve in Figure 10 is comparable to the case where χ_{BS} = 0.0 and h_b = 10 (Figure 7).

Increasing the height of the bump further enhances the effective surface area, providing additional sites for chain attachment along the vertical face of the bump. Now, when one end of the chain binds to a ridge, the other end may bind to the side of the same bump. Consequently, there may be fewer chains that span the wells.

When the bump height is raised to 20 lattice sites, h_s remains equal to 5, and the degree of planarization is now improved to 0.75. However, the uniformity of the film within the average layer thickness is reduced from that evidenced in the h_b = 10 case. Thus, in terms of effectively decreasing the overall surface roughness, the case where χ_{BS} = 1.0 and h_B = 10 proves to be the most effective.

In order to further investigate the uniqueness of the ABA copolymers in planarizing the rough surface, we compared these results with results obtained from simulations of the adsorption of a homopolymer on the same rough surface with h_b equal to 10. Here, all sites along the chain are equivalent. In order to model this simpler scenario, we adopted a standard Metropolis algorithm for the simulation.[14] Thus, the probability that a chain will bind to the surface is now given by $s = \exp(-n_P\chi_{PS})/(1 + \exp(-n_P\chi_{PS}))$, where n_P is the number of polymer sites that are in contact with the surface and χ_{PS} is the polymer–surface interaction energy. The values of χ_{PS} are chosen to be less than or equal to zero, modeling an attractive polymer–surface interaction when χ_{PS} is negative and a neutral interaction when χ_{PS} equals zero. (If the homopolymer–surface interaction were repulsive, there would be no gain in energy and, thus, no driving force for the chain to bind onto the surface.)

The conformation of the adsorbed chains will clearly depend on the magnitude of χ_{PS}, and this is a topic that will be explored in a future article. Here, we will examine the case where χ_{PS} = −1.0 and the chain length equals 50 lattice sites. The resulting SDD in the Z direction is narrower than that for the copolymer case, and the average layer thickness is approximately three layers (Z = 12–14). Figure 11 shows the SDD along the Y direction for this film. The average polymer density in this volume is 57%

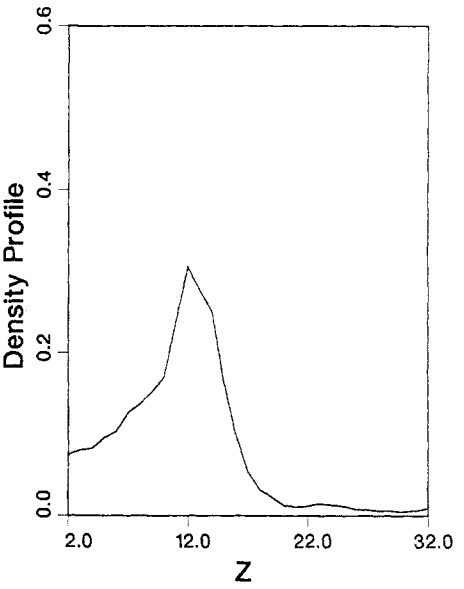

Figure 12. SDD in the Z direction for N = 30 from the reversible binding model.

and d = 0.8. As both this d value and the figure show, the film is far less uniform than that produced by the copolymer in Figure 9. Most importantly, by comparing these two figures, we see that the bridging in the region between the wells is significantly reduced in the case of the homopolymer.

These results indicate that a copolymer, where some beads are attracted to the surface while a large block is more attracted to the solvent, provides the optimal polymer architecture for spanning the ridges of a rough surface.

Finally, we examine the effect of reversible binding on the adsorption behavior. In particular, we set P, the probability that the chain can desorb from the surface, equal to 0.5 for the chains that are bound at only one end and to 0.1 for chains attached through both A ends. (Here, we assumed that desorption is more facile if the chain is bound through only one A block.) In addition, we set N equal to 30. Figure 12 shows the SDD in the Z direction under these conditions. A comparison between this figure and the appropriate curve from the irreversible binding model (solid line in Figure 5) reveals the significant effect

of reversible polymer–surface adsorption. As can be seen, the polymer density in the wells is greater in the case of reversible binding. When adsorbed chains can break away from the surface, some will continue to diffuse toward the bottom plane and, subsequently, bind within the wells. This effect should also be apparent for the shorter chain lengths. Further comparison of the solid line in Figure 5 and Figure 12 shows that there are no dramatic differences between the curves above the $Z = 12$ plane. Thus, the predominant effect of reversibility is to enhance the polymer density in the well volume.

Conclusions

We have shown that adsorbing ABA triblock copolymer chains can bind to neighboring ridges on a rough surface and thereby span the intervening well if a number of conditions are satisfied. These conditions are as follows: (1) the mean end-to-end distance of the chain is comparable to the well width; (2) the chain has a copolymer architecture where short "sticky" A units lie at each end of the intervening B block; and (3) the A-surface interaction is highly attractive while the B-surface interaction is repulsive.

Such copolymers are more efficient than homopolymers at planarizing a rough surface. These findings advance our understanding of the adsorption process on rough surfaces and are of technological significance to the preparation of thin films, coatings, and adhesives.

Acknowledgment. A.C.B. gratefully acknowledges financial support from the National Science Foundation, through Grant DMR-8718899, the Union Carbide Corp., and PPG Industries.

References and Notes

(1) Hone, D.; Ji, H.; Pincus, P. A. *Macromolecules* **1987**, *20*, 2543.
(2) Ji, H.; Hone, D. *Macromolecules* **1988**, *21*, 2600.
(3) Douglas, J. F. *Macromolecules* **1989**, *22*, 3707 and references therein.
(4) (a) Munch, M.; Gast, A. *Macromolecules* **1988**, *21*, 1366. (b) Marques, C.; Joanny, J. F.; Liebler, L. *Macromolecules* **1988**, *21*, 1051. (c) Citations 1–9 in ref 1 above.
(5) Balazs, A. C.; Lewandowski, S. *Macromolecules* **1990**, *23*, 839.
(6) Ghandi, S. K. *VLSI Fabrication Principles, Silicon and Gallium Arsenide*; John Wiley and Sons: New York, 1983.
(7) Verdier, P. H.; Stockmayer, W. H. *J. Chem. Phys.* **1962**, *36*, 227.
(8) Hilhorst, H. J.; Deutch, J. M. *J. Chem. Phys.* **1975**, *63*, 5153.
(9) (a) Granick, S. American Physical Society Meeting, March 1989, High Polymer Physics Division, Poster Session. (b) Tirrell, M., private communication.
(10) (a) Balazs, A. C.; Gempe, M.; Brady, J. *J. Chem. Phys.* **1990**, *92*, 2036. (b) Kolb, M. *J. Phys. A.* **1986**, *19*, L263.
(11) Balazs, A. C.; Hu, J. Y.; Lentvorki, A. P.; Lewandowski, S.; Lantman, C. *Phys. Rev. A* **1990**, *41*, 2109.
(12) Tassin, J. F.; Siemens, R. L.; Tang, W. T.; Hadziioannou, G.; Swalen, J. D.; Smith, B. A. IBM Research Report RJ 6252 (61649), 1988.
(13) Rothman, L. B. *J. Electrochem. Soc.* **1980**, *127*, 2216.
(14) Binder, K.; Heermann, D. W. *Monte Carlo Simulation in Statistical Physics*; Springer-Verlag: Berlin, 1988; p 18.